

## Evaluation of body weight of sea cucumber *Apostichopus japonicus* by computer vision\*

LIU Hui (刘辉)<sup>1,2</sup>, XU Qiang (许强)<sup>1,\*\*</sup>, LIU Shilin (刘石林)<sup>1</sup>, ZHANG Libin (张立斌)<sup>1</sup>,  
YANG Hongsheng (杨红生)<sup>1,\*\*</sup>

<sup>1</sup> Key Laboratory of Marine Ecology and Environmental Sciences, Institute of Oceanology, Chinese Academy of Sciences, Qingdao 266071, China

<sup>2</sup> University of Chinese Academy of Sciences, Beijing 100049, China

Received Apr. 7, 2014; accepted in principle May 28, 2014; accepted for publication Jun. 24, 2014

© Chinese Society for Oceanology and Limnology, Science Press, and Springer-Verlag Berlin Heidelberg 2015

**Abstract** *Apostichopus japonicus* (Holothuroidea, Echinodermata) is an ecological and economic species in East Asia. Conventional biometric monitoring method includes diving for samples and weighing above water, with highly variable in weight measurement due to variation in the quantity of water in the respiratory tree and intestinal content of this species. Recently, video survey method has been applied widely in biometric detection on underwater benthos. However, because of the high flexibility of *A. japonicus* body, video survey method of monitoring is less used in sea cucumber. In this study, we designed a model to evaluate the wet weight of *A. japonicus*, using machine vision technology combined with a support vector machine (SVM) that can be used in field surveys on the *A. japonicus* population. Continuous dorsal images of free-moving *A. japonicus* individuals in seawater were captured, which also allows for the development of images of the core body edge as well as thorn segmentation. Parameters that include body length, body breadth, perimeter and area, were extracted from the core body edge images and used in SVM regression, to predict the weight of *A. japonicus* and for comparison with a power model. Results indicate that the use of SVM for predicting the weight of 33 *A. japonicus* individuals is accurate ( $R^2=0.99$ ) and compatible with the power model ( $R^2=0.96$ ). The image-based analysis and size-weight regression models in this study may be useful in body weight evaluation of *A. japonicus* in lab and field study.

**Keyword:** *Apostichopus japonicus*; wet weight; computer vision; support vector machine

### 1 INTRODUCTION

*Apostichopus japonicus* (Holothuroidea, Echinodermata) — a temperate benthic species found on sandy and muddy-sand substrates as well as rocky shores along the Asian coast (Choe and Ohshima, 1961) — is an important economic fishery resource in China, Japan, and South Korea (Yang et al., 2005). Wherein, aquaculture production of sea cucumber in China reached 170 kilotons in 2012 (China Fishery Statistical Year Book, 2013).

Obtaining precise measurements of the body size of this species is an essential aspect of monitoring growth of breeding *A. japonicus* population as well as determining the structure of a wild population (Watanabe et al., 2012). However, size measurements of this species are difficult due to large variation in

body shape and length of the species. Body weight of sea cucumbers is highly variable because of variation in the quantity of water in the respiratory tree and intestinal content of this species. Currently, the two most accurate methods for determining the size of this species are to anaesthetize specimens prior to measurement (Yamana et al., 2005) or to weigh specimens after the removal of internal organs and body fluids (Choe, 1963). Neither of these two

\* Supported by the National Natural Science Foundation of China (NSFC)-Shandong Joint Fund for Marine Science Research Centers (No. U1406403), the National Key Technology Research and Development Program of China (No. 2011BAD13B02), the National Marine Public Welfare Research Project (No. 201205023), the Strategic Priority Research Program of Chinese Academy of Sciences (No. XDA11020404)

\*\* Corresponding authors: xuqiangcas@126.com; hshyang@126.com

methods is suitable for studies in a field survey. The current method used in the field surveys is to collect individual samples by diving, after which specimens are weighed on board a ship or on land (Qin et al., 2009; Sun et al., 2012).

Machine vision is a sophisticated inspection technology, used in the aquaculture industry and field surveys, that has the capacity to carry out size and weight predictions of aquatic products (Gümüş et al., 2011; Zion, 2012). The main processes involved in size and weight predictions include the following: image capturing, image processing, and the development of a prediction model. An exponential model was used for the regression of fish weight and fish body area, extracted using image processing in fish species such as the Alaskan pollock (*Theragra chalcogramma*) (Balaban et al., 2010) and rainbow trout (*Oncorhynchus mykiss*) (Gümüş and Balaban, 2010). In both of these studies,  $R^2$  reached up to 0.99. A support vector machine (SVM) was used to predict the fish weight using 13 dimensional morphological parameters of images of the side and the top view of the fish, with an accuracy of up to 97% (Odone et al., 2001). The 13 dimensional morphological parameters included 7 parameters (area, perimeter, length, the ratio area/length, the ratio area/perimeter, the minimum width, the maximum width) from side view, and 6 parameters (all parameters above except minimum width) from top view. Stereo-video can be used to estimate the body length of fish when it is not possible to ascertain the fish position and the distance between the fish and the camera, information that is normally needed to predict the weight of individual fish (Harvey et al., 2002; Torisawa et al., 2011). A three-dimensional point-distribution model, which considered the strength of an edge and its proximity to attract landmarks to edges, was modified for body length predictions, with an accuracy of up to 95% (Tillett et al., 2000). The dimension and weight prediction of oysters (Damar et al., 2007) as well as the auto grading of scallop (Lin et al., 2006) can be also achieved by machine vision. A visual mechanical system was also designed to classify and pack up shrimp through studying the relationship between the size and weight of the shrimp. Although machine vision is a useful and efficient technology in weight prediction and field survey, it has not been frequently used in the study of *A. japonicus*.

SVM is a supervised learning method that is widely used for both statistical classification and regression analysis (Cristianini and Shawe-Taylor, 2000; Vapnik, 2000). It maps the vector sets which are usually difficult

to divide in low dimensional space to high dimensional space, and construct a decision surface, called hyper-plane. The data points closest to the hyper-plane called support vectors. It has many advantages when used for small-sample, nonlinear high-dimensional pattern recognition (Mukherjee et al., 1997; Sebald and Bucklew, 2000). In our study, we attempted to use multi-dimensional morphological parameters of *A. japonicus* to build an SVM model to predict the wet weight of *A. japonicus* in different flexible states.

This study aims to: (1) establish thorn removing method from *A. japonicus* images and obtaining morphological parameters of individual *A. japonicus*; (2) to use SVM to build a wet weight prediction model for *A. japonicus* and to test this model; (3) to compare the accuracy of the SVM model with that of the power model.

## 2 MATERIAL AND METHOD

### 2.1 Sample preparation

The *A. japonicus* individuals used in this experiment were from an *A. japonicus* farm in Shandong Province, China. Prior to the experiment, *A. japonicus* specimens had been maintained in laboratory facilities for 24 hours to facilitate defecation. Samples were squeezed softly to expel water from the respiration tree, and the surface of *A. japonicus* individuals was wiped with absorbent paper. The wet weight of *A. japonicus* was determined using an electronic scale (to an accuracy of 0.01 g). We selected 33 *A. japonicus* individuals for research, 18 of which weighed less than 50 g, with the weight of the remaining 15 individuals being in the 50–100 g range.

### 2.2 Image capture system

The image capture system used for *A. japonicus* is illustrated in Fig.1. This system is comprised of three parts: the image capture platform, the illumination system, and the image pick-up system.

#### 2.2.1 Illumination system

Six LED soft rope lights were placed at the bottom of the image capture system (Fig.1) to provide lighting from down to up. The illumination system caused significant contrast of image with advantage in the image processing. The image capture processes were all performed in a dark room.

#### 2.2.2 Image capture platform

A flat acrylic optics diffuser plate (60 cm×40 cm) was placed into a glass aquarium (60 cm×40 cm×

20 cm). Fresh seawater was poured over the optics diffuser plate to a depth of about 15 cm. The acrylic optics diffuser plate was laid on the bottom of the water to achieve brightness uniformity when the LED ray penetrated the plate. During image capture, *A. japonicus* individuals were placed onto the optics diffuser plate, in order to capture a strong-contrast image. Our aim is to simulate a seawater environment, to ensure that the *A. japonicus* specimens were able to maintain a normal body state and to move in their normal free-creeping style, in order to obtain images of these animals in their various flexible states.

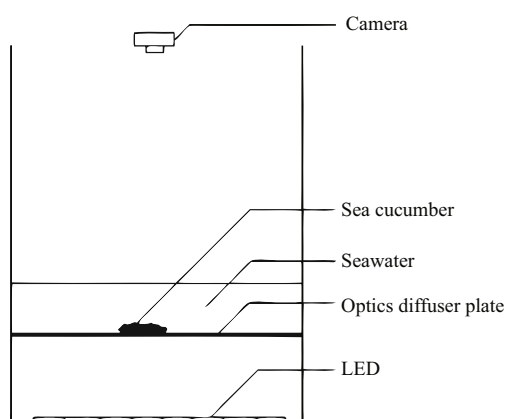


Fig.1 The image capture system used for *A. japonicus*

### 2.2.3 Image pick-up system

We used a CCD camera (Canon G12) to take photos vertically downwards, to obtain images of the dorsal surface of *A. japonicus* in different flexible states. The camera was placed at a distance of about 80 cm from the image capture platform. The image was in RGB format, with a resolution of 3 648×2 736 pixels.

The *A. japonicus* individuals were placed into the glass container and when they started to move, the G12 camera was set to continuous capturing mode (at a rate of 2 pieces per second). 100 photos for each *A. japonicus* were taken.

## 3 IMAGE PROCESSING AND ANALYSIS

Image processing includes the following aspects: background segmentation (binary images in which the *A. japonicus* image is separated from the background), morphology processing (obtaining images of the main body parts of *A. japonicus*) and feature extraction (obtaining morphological parameters of *A. japonicus*). Image processing and analysis were both realized in Matlab 7.12.0 (MathWorks, Inc.).

### 3.1 Background segmentation

To obtain a size estimate and weight prediction of *A. japonicus*, morphologic parameters relevant to

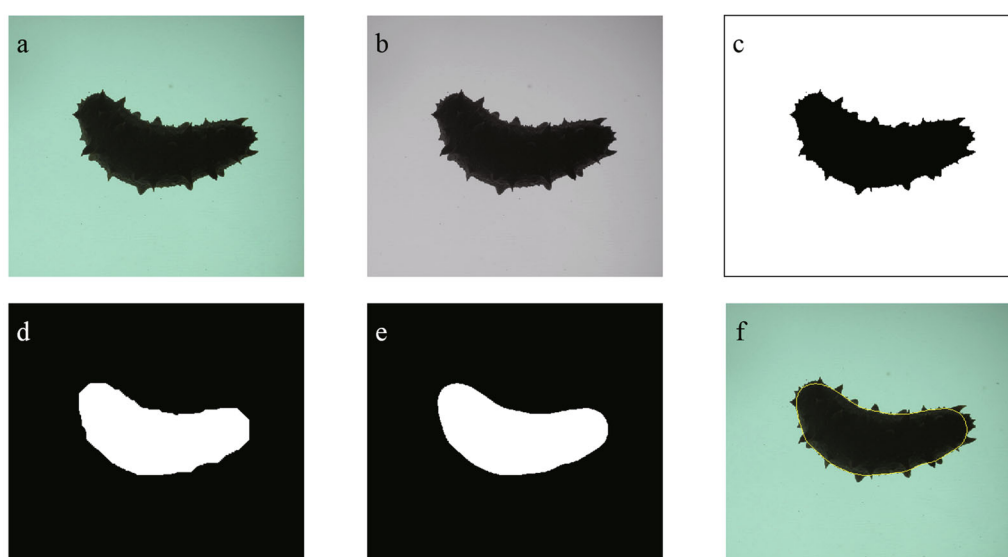
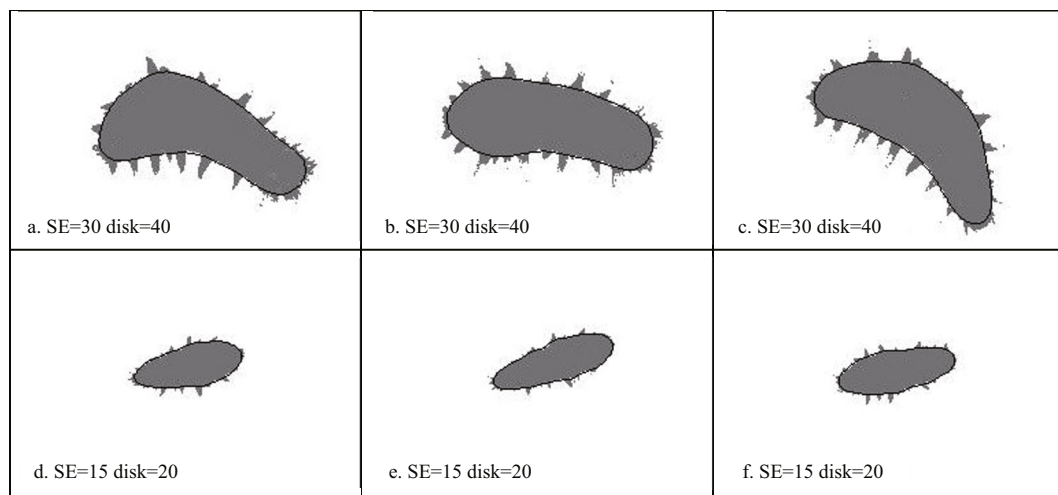


Fig.2 The image processing and feature extraction of *A. japonicus*

a. Original image; b. grayscale image; c. binary image; d opening operation; e. smoothing filtering; f. edge detection.



**Fig.3 SE and disk setting of two *A. japonicus* specimens of different sizes**

The pixel size in all the six images was  $250 \times 170$ . a–c and d–f respectively represent different body shapes of two *A. japonicus* individuals. The (SE=30; disk=40) parameter was adopted in a–c while the (SE=15; disk=20) was adopted in d–f.

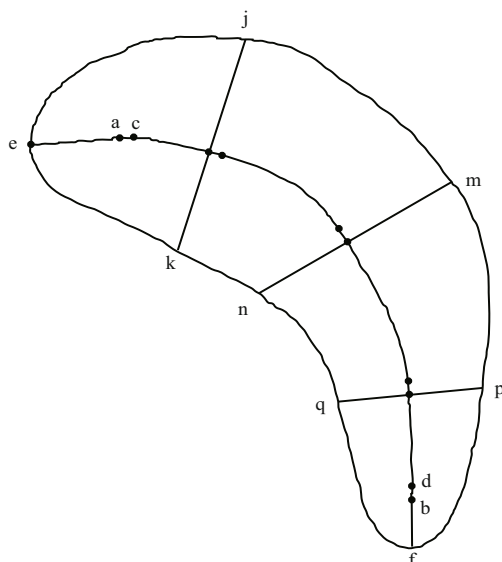


**Fig.4 Extraction of body length and body breadth of *A. japonicus***

individual size were required. The RGB format (Fig.2a) was transformed to a grayscale map (Fig.2b) which was then transformed to binary image (Fig.2c) by gray threshold conversion.

### 3.2 Morphological processing

The main task of image morphological processing was to remove noise in images as well as the thorn images of *A. japonicus*, thereby obtaining an image of the body core of *A. japonicus*.

Some noise points in the image may remain after background segmentation. An opening operation was therefore conducted, to get rid of these noise points in the binary image. After the removal of noise points,

the thorns can be segmented, by performing another opening operation and mean-smoothing filtering in the circular area (Fig.2e). Different-sized thorns were found in different specimens of *A. japonicus*. Therefore, for each individual *A. japonicus*, the structure element parameters of opening operation (SE) and the smooth filtering parameters of mean filtering in the circular area (disk) were set according to the size of the thorn. Generally, the larger specimens were provided with a larger SE and disk, smaller sized specimens were provided with a smaller SE and disk. The same opening operation and filtering parameters can be adopted for same-sized specimens.

### 3.3 Feature extraction

The features that needed to be extracted included area, perimeter, body length, and body breadth at the quarter spot of body length.

Connected domain detection was carried out on the morphologically processed binary image and the area  $A$  and the perimeter  $P$  were extracted.

After morphological processing, the image was thinned to obtain a curve  $ab$  (Fig.4) with a width of 1 pixel. The point defined by  $c$  and  $d$ , which was 10 pixels away from the two endpoints on the curve  $ab$ , was found, and the slope of the curves  $ac$  and  $bd$  was calculated, to extend curves  $ca$  and  $db$  to enable an intersection with the outline of *A. japonicus*, to obtain the complete body length curve  $ef$ .

The body length curve  $ef$  was divided into four equal parts. The normal on the three equally-divided points intersected with the outline, to obtain three body breadths:  $jk$ ,  $mn$ , and  $pq$  (Fig.4).

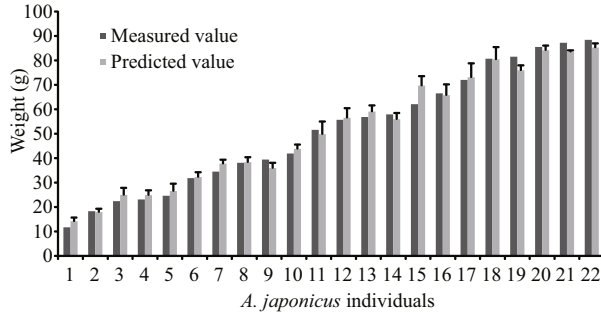


Fig.5 Measured value and predicted value of each of 22 individuals in the train set ( $R^2=0.994$ )

## 4 RESULT

### 4.1 SVM and power model development

#### 4.1.1 Datasets for training and testing SVM

During the experiment, we chose ten images to represent the different body shapes of every *A. japonicus* individual. For each image, the parameters included the current body length  $L$ , three body breadths  $B_f$ ,  $B_m$ ,  $B_b$ , the perimeter  $P$ , the area  $A$ , the product of the body length and the three body breadths  $L \times B_f$ ,  $L \times B_m$ ,  $L \times B_b$ , and the ratio of breadths  $B_f/B_m$ ,  $B_f/B_b$  were obtained. This generated 11 dimensional data in 330 groups. Data from 220 groups were used for SVM model training, and data from 110 groups for model testing.

Prior to SVM training, data dimension normalization was conducted by linear mapping  $[-1, 1]$  of every one-dimensional dataset, after which PCA dimension reduction was performed. The feature table contained 330 samples and 11 attributes.

#### 4.1.2 SVM training and testing

SVM was realized in LibSVM library and the RBF kernel function was selected. RBF kernel function  $K(x, y) = \exp(-\gamma \|x - y\|^2)$ ,  $\gamma > 0$  can map the sample to higher dimensional space and can be used for dealing with examples in which the relationship between current class labels and features is non-linear. We therefore utilized the radial basis function kernel and the set the parameter epsilon (tolerance of termination criterion) to 0.01. A K-fold cross validation and grid search was used for the optimization procedure of penalty factor  $C$  and kernel parameter  $\gamma$ . For the grid search, K-CV cross validation was used to obtain a  $C$  (log2-range: -8 to 8 step 0.5) and  $\gamma$  (log2-range: -8 to 8, step 0.5) training set. Group  $(C, \gamma)$ , with the highest accuracy rate, was chosen for the optimal parameter. This will be used later, for training in SVM.

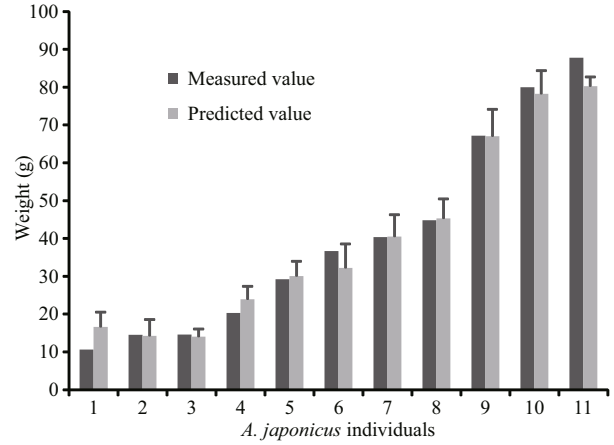


Fig.6 Model training results  $R^2=0.994$

#### 4.1.3 SVM and power model performance evaluation

We used RMSE (root mean square error),  $R^2$  (the square of correlation coefficient) and relative errors (RE) to evaluate the SVM performance.  $R^2$  was used to evaluate the power model.

$$\text{RMSE} = \left( \frac{1}{l} \sum_{i=1}^l (f(x_i) - y_i)^2 \right)^{0.5}, \quad (1)$$

$$R^2 = \frac{\left( \bar{l} \sum_{i=1}^l f(x_i) y_i - \sum_{i=1}^l f(x_i) \sum_{i=1}^l y_i \right)^2}{\left( \bar{l} \sum_{i=1}^l f(x_i)^2 - \left( \sum_{i=1}^l f(x_i) \right)^2 \right) \times \frac{1}{\left( \bar{l} \sum_{i=1}^l y_i^2 - \left( \sum_{i=1}^l y_i \right)^2 \right)}}, \quad (2)$$

$$\text{RE} = \frac{1}{l} \sum_{i=1}^l \frac{f(x_i) - y_i}{y_i} \times 100\%, \quad (3)$$

where  $y_i$  is the measured value of the wet weight of *A. japonicus*,  $x_i$  is the morphological parameter, and  $f(x_i)$  is the model prediction value of the wet weight.

RMSE is used to show the difference between the measured value and the model prediction value of the wet weight. The lower the value, the better the SVM performance.  $R^2$  within the range of 0 to 1, is the statistical index to illustrate the close relationship degree of the variables. The larger the value of  $R^2$  the better the regression result. RE is the relative error, and the smaller the value of RE, the better the regression result will be.

### 4.2 SVM performance

The performance of SVM model in train and test processes, is illustrated in Figs.5 and 6. Average values of the predicted weights of ten pictures of each *A. japonicus* specimen and the actual measured values



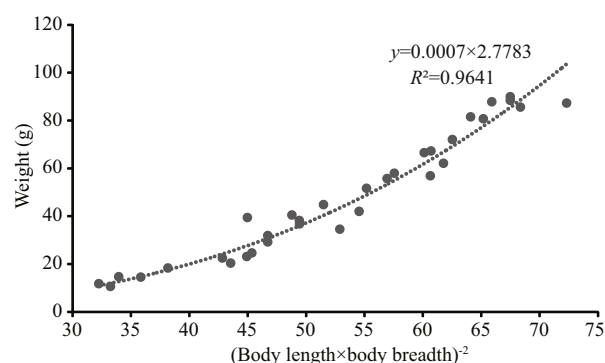


**Fig.7 Power model (body length×body breadth)<sup>2</sup> with weight  $R^2=0.964$**

were plotted, and their correlation calculated.  $R^2$  of the model building set was 0.99, and  $R^2$  of model testing set was 0.98. Root-mean-square errors (RMSE) and the relative RE were respectively calculated for *A. japonicus* in different weight ranges. RMSE values of *A. japonicus* individuals 0–50 g and 50–100 g in the train set were 2.13 g and 3.26 g, with RE being 5.28% and 0.46%, respectively. In the test set, the RMSE values of *A. japonicus* individuals 0–50 g and 50–100 g were 2.99 g and 4.48 g, respectively, with RE obtaining 7.69% and 3.67%.

### 4.3 Power model performance

The average  $\sqrt{L \times B_m}$  of each *A. japonicus* individual and the measured weight was fitting with the power model  $W = 7 \times 10^{-4} \times \sqrt{L \times B_m}^{2.7783}$  ( $R^2=0.964$ ), where  $W$  was measured in grams.  $L$  and  $B_m$  are measured in mm.

## 5 DISCUSSION

Unlike most fish species, in which the body shape is relatively stable, *A. japonicus* undergoes more changes to its body shape, due largely to its ability for extension and contraction. In our study, the *A. japonicus* individuals were placed in seawater in a situation in which free crawling was possible. Images of *A. japonicus* individuals were captured continuously, contracting and extending. Features associated with different body shapes of each individual were noted and extracted, then regress with the corresponding weight value. The body weight of *A. japonicus* is variable, depending on the amount of water in the respiration tree and intestinal content. In this study, *A. japonicus* individuals had been bred for a period, to allow for defecation, and water in the respiration tree was discharged through squeezing, as much as possible, to reduce the weight variation and

to obtain a stable weight value. This method of weighing was also used in the field population survey.

Thorn removal was a necessary step in image processing, because the existence of thorns results in a higher available of body length and breadth. An opening operation and mean smoothing filtering were employed to remove the thorns. The structure element parameters of the opening operation (SE) and the smooth filtering parameters of mean filtering in the circular area (disk) were set artificially, according to the size of the thorn. After thorn removal, body length extracting was realized through image thinning. This method has been used for other aquatic food size estimations. Body color is an important characteristic for *A. japonicus* with high concern in aquaculture industry. In our study, all the image captured were transformed to grayscale and the color was ignored.

Because of the morphological flexibility of *A. japonicus*, the commonly-used indexes of other species—such as body length and body area—have no obvious correlation with weight. A power model was used in the weight regression of *A. japonicus*, and a strong correlation was found between weight and  $\sqrt{L \times B}$ , which was an average of 200 measurements for each individual (Yamana and Hamano, 2006). In our study, the extraction of body length and body breadth was achieved using image processing; and  $\sqrt{L \times B}$  with weight in the power model was test. The  $R^2$  of the power model was 0.964. Besides body length and body breadth, area and perimeter were also referred in SVM in this study, with  $R^2$  being equal to 0.994 in both train set and test set. In this study, SVM referred more parameters and achieved more accuracy.

## 6 CONCLUSION

In this research, we removed thorns and extracted area, perimeter, body length and body breadth of *A. japonicus* images through image processing, and built a predictive model of *A. japonicus* weight, using SVM and a power model. The SVM model ( $R^2=0.994$ ) and power model ( $R^2=0.964$ ) perform well in terms of weight predictions of *A. japonicus*. Further work will be required to obtain the number of thorns and color of *A. japonicus* using computer vision.

### References

- Balaban M O, Chombeau M, Cırbacı D, Gümüş B. 2010. Prediction of the weight of Alaskan Pollock using image analysis. *Journal of Food Science*, **75**(8): E552-E556.
- Bureau of Fisheries, Ministry of Agriculture of China. 2013. China Fishery Statistical Year Book. China Agriculture Press, Beijing, China. p.29. (in Chinese)

- Choe S, Ohshima Y. 1961. On the morphological and ecological differences between two commercial forms, "Green" and "Red", of the Japanese common sea cucumber, *Stichopus japonicus* Selenka. *Bulletin of the Japanese Society of Scientific Fisheries*, **27**(2): 97-106.
- Choe S. 1963. Namako no kenkyu. Biology of the Japanese Common Sea Cucumber *Stichopus japonicus* (Selenka). Kaibundo, Tokyo. (in Japanese with English abstract)
- Cristianini N, Shawe-Taylor J. 2000. An Introduction to Support Vector Machines and Other Kernel-Based Learning Methods. Technische Universitat Darmstadt, Cambridge University Press.
- Damar S, Yagiz Y, Balaban M, Ural S, Oliveira A, Crapo C. 2007. Prediction of oyster volume and weight using machine vision. *Journal of Aquatic Food Product Technology*, **15**(4): 3-15.
- Gümüş B, Balaban M Ö, Ünlüsayın M. 2011. Machine vision applications to aquatic foods: a review. *Turkish Journal of Fisheries and Aquatic Sciences*, **11**: 171-181.
- Gümüş B, Balaban M O. 2010. Prediction of the weight of aquacultured rainbow trout (*Oncorhynchus mykiss*) by image analysis. *Journal of Aquatic Food Product Technology*, **19**(3-4): 227-237.
- Harvey E, Fletcher D, Shortis M. 2002. Estimation of reef fish length by divers and by stereo-video: a first comparison of the accuracy and precision in the field on living fish under operational conditions. *Fisheries Research*, **57**(3): 255-265.
- Lin A, Sun B, Yada S. 2006. Studies on the detecting method of scallop grading based on machine vision. *Journal of Fisheries of China*, **30**(3): 397-403. (in Chinese with English abstract)
- Mukherjee S, Osuna E, Girosi F. 1997. Nonlinear prediction of chaotic time series using support vector machines. *Neural Networks for Signal Processing [1997] VII. Proceedings of the 1997 IEEE Workshop*. p.511-520.
- Odone F, Trucco E, Verri A. 2001. A trainable system for grading fish from images. *Applied Artificial Intelligence*, **15**(8): 735-745.
- Qin C, Dong S, Tan F, Tian X, Wang F, Dong Y, Gao Q. 2009. Optimization of stocking density for the sea cucumber, *Apostichopus japonicus* Selenka, under feed-supplement and non-feed-supplement regimes in pond culture. *Journal of Ocean University of China*, **8**(3): 296-302.
- Sebald D J, Bucklew J A. 2000. Support vector machine techniques for nonlinear equalization. *Signal Processing, IEEE Transactions on*, **48**(11): 3 217-3 226.
- Sun Z-L, Gao Q-F, Dong S-L, Shin P K, Wang F. 2012. Estimates of carbon turnover rates in the sea cucumber *Apostichopus japonicus* (Selenka) using stable isotope analysis: the role of metabolism and growth. *Marine Ecology Progress Series*, **457**: 101-112.
- Tillett R, McFarlane N, Lines J. 2000. Estimating dimensions of free-swimming fish using 3D point distribution models. *Computer Vision and Image Understanding*, **79**(1): 123-141.
- Torisawa S, Kadota M, Komeyama K, Suzuki K, Takagi T. 2011. A digital stereo-video camera system for three-dimensional monitoring of free-swimming Pacific bluefin tuna, *Thunnus orientalis*, cultured in a net cage. *Aquatic Living Resources*, **24**(02): 107-112.
- Vapnik V. 2000. The Nature of Statistical Learning Theory. Series: Information Science and Statistics. Originally published as a monograph. 2nd edn. XIX, 314 p. Springer.
- Watanabe S, Zarate J M, Sumbing J G, Lebata-Ramos M J H, Nievaes M F. 2012. Size measurement and nutritional condition evaluation methods in sandfish (*Holothuria scabra* Jaeger). *Aquaculture Research*, **43**(6): 940-948.
- Yamana Y, Hamano T, Yamamoto K-I. 2005. Anesthetizer of the adult sea cucumber *Apostichopus japonicus*. *Nippon Suisan Gakkaishi*, **71**(3): 299-306.
- Yamana Y, Hamano T. 2006. New size measurement for the Japanese sea cucumber *Apostichopus japonicus* (Stichopodidae) estimated from the body length and body breadth. *Fisheries Science*, **72**(3): 585-589.
- Yang H, Yuan X, Zhou Y, Mao Y, Zhang T, Liu Y. 2005. Effects of body size and water temperature on food consumption and growth in the sea cucumber *Apostichopus japonicus* (Selenka) with special reference to aestivation. *Aquaculture Research*, **36**(11): 1 085-1 092.
- Zion B. 2012. The use of computer vision technologies in aquaculture — a review. *Computers and Electronics in Agriculture*, **88**: 125-132.